

Electrodisintegration of ${}^6\text{Li}$ Studied with the Reaction ${}^6\text{Li}(e,e'p)$

J. B. J. M. Lanen,⁽¹⁾ A. M. van den Berg,⁽¹⁾ H. P. Blok,^(2,3) J. F. J. van den Brand,⁽²⁾ C. T. Christou,⁽⁴⁾ R. Ent,^(2,3) A. G. M. van Hees,⁽¹⁾ E. Jans,⁽²⁾ G. J. Kramer,⁽²⁾ L. Lapikás,⁽²⁾ D. R. Lehman,⁽⁴⁾ W. C. Parke,⁽⁴⁾ E. N. M. Quint,⁽²⁾ G. van der Steenhoven,^(2,3) and P. K. A. de Witt Huberts^(1,2)

⁽¹⁾*Fysisch Laboratorium, Rijksuniversiteit Utrecht, 3508 TA Utrecht, The Netherlands*

⁽²⁾*Nationaal Instituut voor Kernfysica en Hoge Energifysica (NIKHEF-K), 1009 AJ Amsterdam, The Netherlands*

⁽³⁾*Natuurkundig Laboratorium, Vrije Universiteit, 1007 MC Amsterdam, The Netherlands*

⁽⁴⁾*Department of Physics, The George Washington University, Washington, D.C. 20052*

(Received 10 April 1989)

The ${}^6\text{Li} \rightarrow p + (n\alpha)$ spectral function for the proton-knockout reaction ${}^6\text{Li}(e,e'p)$ has been measured in parallel kinematics in the missing-momentum range $-100 < p_m < 200$ MeV/c. The data below α breakup are well described by a three-body (anp) model of ${}^6\text{Li}$. The shell model with discrete energy eigenstates cannot describe the data. The experimental spectroscopic strength below α breakup amounts to 0.79(10), compared to 0.87 as predicted by the three-body model and 1.33 as calculated from a schematic harmonic-oscillator shell model. The discrepancy between the predictions of the two models is discussed.

PACS numbers: 25.30.Fj, 21.10.Jx, 27.20.+n

The nucleus ${}^6\text{Li}$ constitutes a transitional case between few-body systems for which exact calculations can be performed with the Faddeev technique and heavier nuclei whose static and dynamic properties are commonly described in the shell-model approximation. Theoretical models for the structure of ${}^6\text{Li}$ usually follow either the shell-model or the three-body approach. In nuclei with $A \geq 12$, recent $(e,e'p)$ data have shown appreciable quenching of the single-particle strength relative to the shell-model estimate,¹⁻³ whereas such a quenching is not observed for ${}^3\text{He}$ and ${}^4\text{He}$.^{4,5} Hence the ${}^6\text{Li}(e,e'p)$ data upon comparison with shell-model and three-body calculations may provide a clue as to the mechanism for this quenching in heavier nuclei.

A few ${}^6\text{Li}(p,2p)$ and ${}^6\text{Li}(e,e'p)$ experiments have been reported.^{6,7} In these data, one has observed the absence of a minimum at zero recoil momentum in the overlap function of ${}^6\text{Li}$ with the final state $p + (n\alpha)$, at variance with the prediction of a pure p -shell model. However, the comparison of the data with theoretical calculations^{6,7} is hampered by distortion effects in the $(p,2p)$ reaction and an inadequate energy resolution in the $(e,e'p)$ experiment. In this paper we present high-resolution spectral-function data extracted from absolute cross sections of the reaction ${}^6\text{Li}(e,e'p)n\alpha$.

The experiment was performed with the electron accelerator MEA and the dual spectrometer setup at NIKHEF-K.⁸ Using an enriched (98.7%) ${}^6\text{Li}$ foil with a thickness of 13.0 mg/cm², $(e,e'p)$ coincidence cross sections were measured in parallel kinematics; i.e., the proton with missing momentum $p_m = p - q$ is knocked out with momentum \mathbf{p} parallel to the electron momentum transfer \mathbf{q} . A range of p_m from -100 to 200 MeV/c was covered by measurements at incident energies of 320 and 480 MeV. The relative (p - ${}^5\text{He}$) kinetic energy in

the center-of-mass system $T_{c.m.}$ was kept constant at 64.8 MeV. The spectral function $S(E_m, p_m)$, i.e., the probability of finding a proton with binding energy E_m and momentum p_m in the target nucleus, was extracted from the coincidence cross section in the standard manner.¹ A missing-energy spectrum integrated in the region $15 < p_m < 65$ MeV/c is shown in Fig. 1. The peak at $E_m = 4.59$ MeV, 0.89 MeV above the ${}^6\text{Li} \rightarrow p + n + \alpha$ separation energy, corresponds to the $J^\pi = \frac{3}{2}^-$ quasibound state of ${}^5\text{He}$, while the one at 21.35 MeV corresponds to the ${}^6\text{Li} \rightarrow p + (d + {}^3\text{H})$ breakup channel with $J^\pi = \frac{3}{2}^+$. The tail from 5 MeV up to 21 MeV is not caused by radiative effects, which were unfolded, but is due to the unbound nature of the residual ($n\alpha$) system. The missing-energy resolution of 120 keV is mainly due to the straggling of protons in the target. By using the ${}^1\text{H}(e,e'p)$ peak due to a small hydrogen contamination

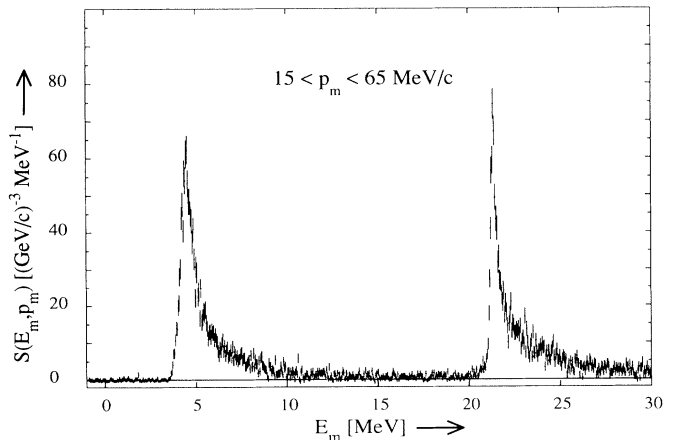


FIG. 1. Missing-energy spectrum of the ${}^6\text{Li}(e,e'p)$ reaction.

of the ${}^6\text{Li}$ target and determining the E_m position of the low-energy edge of the $\frac{3}{2}^+$ excited state, the missing energy was calibrated with an uncertainty of 75 keV. A careful estimate of all experimental uncertainties resulted in a total systematic error on the spectral function of 6% and a 1-MeV/c uncertainty in the determination of p_m .

In Fig. 2 is shown the momentum distribution $\rho(p_m) = \int_{\Delta E} S(E_m, p_m) dE_m$ where the integration is performed over the range $4.1 < E_m < 4.9$ MeV, which includes the main part of the ground state of ${}^5\text{He}$. Besides the statistical uncertainty the error bars also account for the missing-energy uncertainty of 75 keV. The contribution of the radiative tail of the hydrogen contaminant to the data shown in Fig. 2 is less than 1%. For $|p_m| \leq 7.5$ MeV/c the hydrogen tail increases rapidly and therefore the data near $p_m = 0$ MeV/c have been omitted.

Three-body (pna) models^{6,7,9} are used to describe the reaction ${}^6\text{Li}(e, e'p)na$ for relative (n - a) energies below 20 MeV. In the full repulsive model all dominant components of the aN interaction at low energy, i.e., $S_{1/2}$, $P_{1/2}$, and $P_{3/2}$ are used, while the $S_{1/2}$ aN interaction is taken to be purely repulsive. The NN interaction has besides the S contribution also a 4% D -state component. By solving the three-body Schrödinger equation for the

${}^6\text{Li}$ ground state and calculating its overlap amplitude with the $p+(na)$ system, the ${}^6\text{Li}(e, e'p)na$ spectral function can be calculated in the plane-wave impulse approximation (PWIA). The model is formulated in the center-of-mass system, eliminating the need of center-of-mass corrections. Once the two-body interactions are determined, there are *no* free parameters or scale factors to be set in the three-body model.

The solid curve in Fig. 2 represents the theoretical plane-wave momentum distribution $\rho_{\text{PW}}(p_m)$. An unfactorized distorted-wave impulse-approximation (DWIA) calculation with the DWEOPY code¹⁰ has been performed to account for the final-state-interaction (FSI) effects. Since this code needs a bound-state wave function in r space as input, $\rho_{\text{PW}}(p_m)$ has been parametrized with harmonic-oscillator eigenfunctions $\phi_{nl}(p_m)$:

$$\rho_{\text{PW}}(p_m) = \left[\sum_{n=1}^7 a_{n0} \phi_{n0}(p_m) \right]^2 + \left[\sum_{n=1}^7 a_{n1} \phi_{n1}(p_m) \right]^2,$$

where a_{nl} represents the amplitude of the corresponding eigenfunction. As the main contribution to the ${}^6\text{Li} \rightarrow p+(na)$ overlap consists of $l=0$ and $l=1$ partial waves,⁹ only those l values are included in the fit. For the harmonic-oscillator length parameter the value $b=2.03$ fm is adopted.¹¹ It was found that for $n=7$ adequate convergence is obtained.

Four different sets of optical-potential parameters have been used in the FSI calculations. Two sets are derived from p - ${}^4\text{He}$ scattering data measured in the proton energy ranges 31–55 MeV¹² and 85–1240 MeV,¹³ respectively; two other sets are derived from p - ${}^6\text{Li}$ scattering data measured in the proton energy range 14–45 MeV¹⁴ and at 100 MeV,¹⁵ respectively. Except for the latter case, all sets are extrapolated to a value of 78.2 MeV, corresponding to $T_{\text{c.m.}}=64.8$ MeV. The envelope of the four calculated DWIA curves, represented in Fig. 2 by the shaded band, shows that the uncertainty due to the choice of the optical potential is about 5% at low p_m , increasing to 20% at high p_m .

As shown in Fig. 2, the three-body model describes the experimental momentum distribution very well, in particular in the region around $p_m = 0$ MeV/c where the dip structure is nicely reproduced. The nonzero value of $\rho(p_m)$ at $p_m = 0$ MeV/c is due to the na rescattering in the final state in a relative S wave, which has a nonzero overlap with components of the same angular momentum in the ${}^6\text{Li}$ ground-state wave function.⁹

The main features of the shell-model description for ${}^6\text{Li}$ can be understood without performing a sophisticated calculation. In the schematic $0\hbar\omega$ shell model, the ${}^6\text{Li}$ ground-state wave function has a $(0s)^4(0p)^2$ configuration, whose orbital symmetry is represented by the partition [42].¹⁶ Picking up one proton populates ${}^5\text{He}$ states of orbital symmetry [41] or [32] with a total spectroscopic strength of 1.33 and 1.67, respectively. These numbers can be obtained by counting the Young ta-

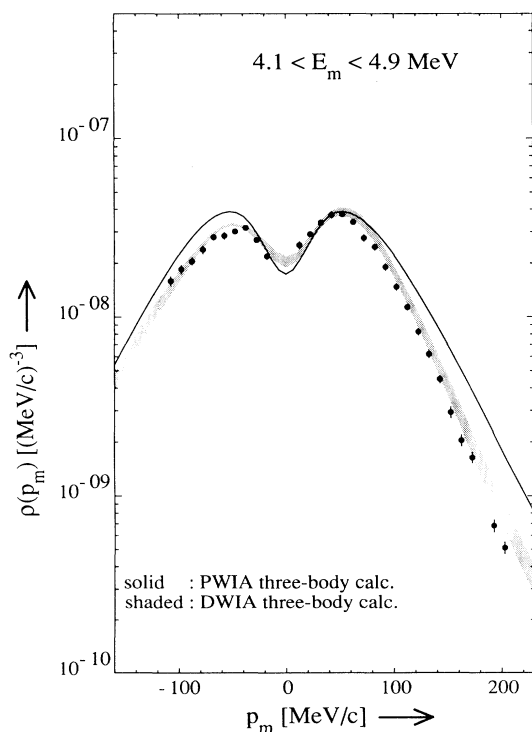


FIG. 2. Momentum distribution for the ${}^6\text{Li}(e, e'p)$ reaction ($4.1 < E_m < 4.9$ MeV). The solid curve represents the results of a PWIA calculation in the three-body model of Ref. 9. The shaded band represents the range of DWIA calculations for four different optical potentials.

bleaus¹⁶ that correspond to the above-mentioned partitions. The spectroscopic strength for the knockout of a proton from the p shell, leaving ${}^5\text{He}$ in a $[41]$ partition, amounts to 1.2. This value includes the center-of-mass correction factor $A/(A-1)=6/5$.¹⁷ From the remaining strength, i.e., 1.8, a small amount of 0.133 is going to a $\frac{1}{2}^+$ state with orbital symmetry $[41]$. Below about 16.7 MeV of excitation energy the ${}^5\text{He}$ states are expected to be dominantly of $[41]$ orbital symmetry. In $1\hbar\omega$ shell-model calculations^{18,19} a $\frac{1}{2}^+$ state in ${}^5\text{He}$ with almost pure $[41]$ symmetry is calculated at about 8-MeV excitation energy.

In Fig. 3 the three-body and shell-model approaches are compared with the data via the quantity $\rho(p_m) = \int_{\Delta E} S(E_m, p_m) dE_m$, where the integration is performed over the E_m interval below α breakup ($3.7 < E_m < 19.7$ MeV). The three-body calculation agrees well with the data. The shell-model calculation with discrete energy eigenstates is inadequate, although it also predicts a filled-in minimum at $p_m = 0$ MeV/c, due to the presence of the $\frac{1}{2}^+$ state below α breakup.

In Fig. 4 the theoretical PWIA momentum distributions are compared via the sum rule $P(p) = 4\pi$

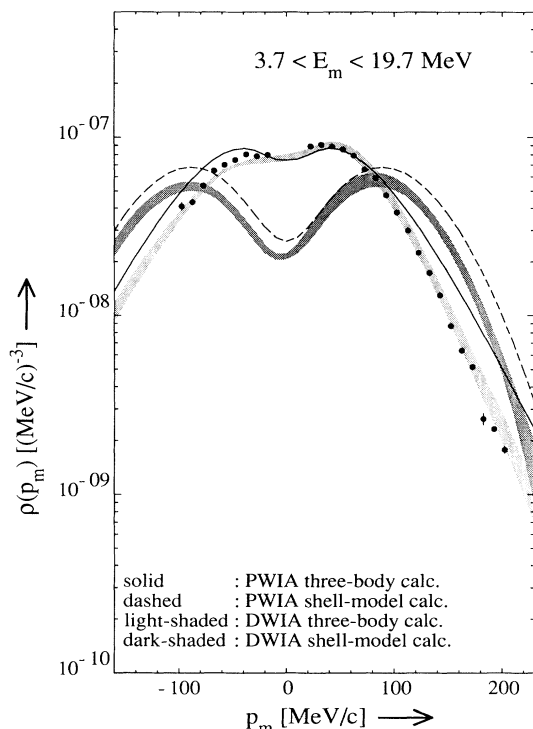


FIG. 3. Momentum distribution for the reaction ${}^6\text{Li}(e, e'p)$ below α breakup ($3.7 < E_m < 19.7$ MeV). The solid and dashed curves represent the results of a PWIA calculation in the three-body model of Ref. 9 and the $0\hbar\omega$ shell model, respectively. The corresponding ranges of DWIA calculations for four different optical potentials are represented by the light- and dark-shaded bands, respectively.

$\times \int_0^p \rho(p_m) p_m^2 dp_m$ which represents the spectroscopic strength. The distortion-corrected experimental data, indicated by the shaded band, encompass the uncertainty in the optical potential and the statistical error. The spectroscopic factor as predicted by the three-body model and the shell model amounts to 0.87 and 1.33, respectively, to be compared with the experimental result of 0.79(10). The error includes the statistical uncertainty and the uncertainty in the extrapolation of the momentum distribution to infinity, estimated to be 4%, the above-mentioned systematical error of 6%, and an uncertainty from the description of the distortion effects, estimated to be 10%.

The spectroscopic factor is well predicted by the three-body model, whereas a considerable quenching is found relative to the shell-model value. We conclude that the shell-model wave functions for ${}^5\text{He}$ and ${}^6\text{Li}$ are not realistic. Other evidence for this stems from the following: (i) Instead of a true continuum wave function for the $A=5$ system, a ${}^5\text{He}$ wave function with discrete energy eigenstates is predicted by the shell model; (ii) the shell model^{18,20} underestimates the experimental root-mean-square charge radius for ${}^6\text{Li}$ by 15%. In the shell model, which correctly takes into account antisymmetrization effects (at the nucleon level), the p -shell radial wave function may therefore overlap too strongly with the s -shell radial wave function. If there were no spatial overlap at all between these s - and p -shell wave functions, the spectroscopic strength for knockout of a p -shell proton would simply be 1.0 instead of 1.2 given by the schematic harmonic-oscillator shell model. In the three-body model, which underestimates the charge radius by only 6%,²¹ the α particle is regarded as structureless and the effect of the antisymmetrization is accounted for in part by the $S_{1/2}$ partial wave of the α - N potential.

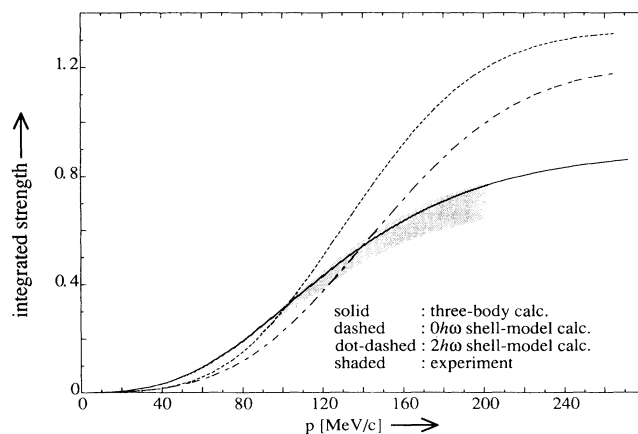


FIG. 4. Sum rule for the spectroscopic strength below α breakup. The solid, dashed, and dot-dashed curves represent the results for the three-body model and the $0\hbar\omega$ and $2\hbar\omega$ shell models, respectively. The shaded band represents the experimental results corrected for FSI effects.

The calculated wave functions presumably become more realistic by increasing the shell-model space. In Fig. 4 the results of a $2\hbar\omega$ shell-model calculation are shown as well. The spectroscopic factor below α breakup amounts to 1.20, a decrease of about 10% with respect to the $0\hbar\omega$ shell-model value. This reduction implies that more strength is to be found beyond α breakup. Based on the value of 0.71 for the spectroscopic factor for the strength below α breakup obtained in an $\{\alpha+d, {}^5\text{He}+p\}$ cluster model,²² whose basis can be described in a very large shell-model space, it is expected that a further increase of the model space would bring down the spectroscopic value considerably.

In summary, the experience in $(e,e'p)$ reactions that few-body models in their description of light systems calculate spectroscopic factors in agreement with the data whereas shell models for heavy nuclei overestimate spectroscopic factors is now acquired for one and the same nucleus, ${}^6\text{Li}$. The three-body (anp) model is quite capable of describing the unbound character of ${}^5\text{He}$ below α breakup. Although also the $0\hbar\omega$ shell model predicts a filled-in minimum at $p_m=0$ MeV/ c for the momentum distribution of the strength below α breakup, it overestimates the spectroscopic factor by 68%. Increasing the shell-model space to $2\hbar\omega$ reduces the spectroscopic factor for the strength below α breakup by 10%.

This work was performed as part of the research program of the Stichting voor Fundamenteel Onderzoek der Materie (FOM) with financial support from the Nederlandse Organisatie voor Wetenschappelijk Onderzoek (NWO). The work of the George Washington University group was supported in part by the U.S. Department of Energy under Grant No. DE-FG05-86-ER40270.

- ¹J. W. A. den Herder *et al.*, Nucl. Phys. **A490**, 507 (1988).
- ²E. N. M. Quint, Ph.D. thesis, University of Amsterdam, 1988 (unpublished).
- ³G. van der Steenhoven *et al.*, Nucl. Phys. **A480**, 547 (1988).
- ⁴E. Jans *et al.*, Nucl. Phys. **A475**, 687 (1987).
- ⁵J. F. J. van den Brand, Ph.D. thesis, University of Amsterdam, 1988 (unpublished).
- ⁶C. T. Christou, D. R. Lehman, and W. C. Parke, Phys. Rev. C **37**, 458 (1988).
- ⁷C. T. Christou, D. R. Lehman, and W. C. Parke, Phys. Rev. C **37**, 477 (1988).
- ⁸C. de Vries *et al.*, Nucl. Instrum. Methods **233**, 1 (1984).
- ⁹C. T. Christou, D. R. Lehman, and W. C. Parke, Phys. Rev. C **37**, 445 (1988).
- ¹⁰C. Giusti and F. Pacati, Nucl. Phys. **A473**, 717 (1987).
- ¹¹T. W. Donnelly and J. D. Walecka, Phys. Lett. **44B**, 330 (1973).
- ¹²G. E. Thompson and M. B. Epstein, Nucl. Phys. **A142**, 571 (1970).
- ¹³W. T. H. van Oers *et al.*, Phys. Rev. C **25**, 390 (1982).
- ¹⁴K. H. Bray *et al.*, Nucl. Phys. **A189**, 35 (1972).
- ¹⁵T. Y. Li and S. K. Mark, Can. J. Phys. **46**, 2645 (1968).
- ¹⁶A. Bohr and B. R. Mottelson, *Nuclear Structure* (Benjamin, New York, 1969).
- ¹⁷A. E. L. Dieperink and T. de Forest, Jr., Phys. Rev. C **10**, 543 (1974).
- ¹⁸A. G. M. van Hees and P. W. M. Glaudemans, Z. Phys. A **314**, 323 (1983).
- ¹⁹A. G. M. van Hees and P. W. M. Glaudemans, Z. Phys. A **315**, 223 (1984).
- ²⁰A. A. Wolters, A. G. M. van Hees, and P. W. M. Glaudemans, Europhys. Lett. **5**, 7 (1988).
- ²¹A. Eskandarian, D. R. Lehman, and W. C. Parke, Phys. Rev. C **38**, 2341 (1988).
- ²²R. Beck, F. Dickmann, and R. G. Lovas, Ann. Phys. (N.Y.) **137**, 1 (1987).